

## Contrasting oxygen and copper isotope effects in $\text{YBa}_2\text{Cu}_4\text{O}_8$ superconducting and normal states

G. V. M. Williams

2. *Physikalisches Institut, Universität Stuttgart, Pfaffenwaldring 57, D-70569 Stuttgart, Germany*  
and *The New Zealand Institute for Industrial Research, P.O. Box 31310, Lower Hutt, New Zealand*

D. J. Pringle

*School of Chemical and Physical Sciences, Victoria University, P.O. Box 31310, Wellington, New Zealand*

J. L. Tallon

*The New Zealand Institute for Industrial Research, P.O. Box 31310, Lower Hutt, New Zealand*

(Received 10 October 1999)

We have used Raman, susceptibility, and  $^{89}\text{Y}$  NMR measurements on the  $\text{YBa}_2\text{Cu}_4\text{O}_8$  superconductor synthesized using pure  $^{63}\text{Cu}$  or  $^{65}\text{Cu}$  to investigate the oxygen and copper isotope effects in  $T_c$  and the normal-state pseudogap. We find no copper or oxygen isotope effects in the normal-state  $^{89}\text{Y}$  Knight shift for temperatures in excess of 150 K. There is a *positive* copper isotope effect in  $T_c$  and, for temperatures less than 150 K, a *negative* copper isotope effect in the normal-state  $^{89}\text{Y}$  Knight shift. This differs from the oxygen isotope effect which is *positive* for both  $T_c$  and the  $^{89}\text{Y}$  Knight shift below 150 K. These results indicate that the normal-state pseudogap may not originate from precursor superconducting pairing.

Isotope effect measurements were of crucial importance in establishing the phonon-induced BCS model of superconductivity.<sup>1</sup> In the weak-coupling BCS model the isotope effect derives from the superconducting transition temperature  $T_c$  being proportional to the Debye temperature. Since the Debye temperature is proportional to  $M^{1/2}$ , where  $M$  is the atomic mass, the isotope-effect coefficient,  $\alpha \equiv -\ln T_c / d \ln M = 0.5$ . The later inclusion of Coulomb repulsion in the pairing interaction resulted in predicted  $\alpha$  values of less than 0.5 and enabled a reasonably good fit to the data where low values of  $\alpha$  correspond to low  $T_c$  values.<sup>2</sup> The situation is more complex in the high-temperature superconducting cuprates (HTSC's), where  $\alpha$  is small near optimal doping and maximum  $T_c$  (Ref. 3) and large for low hole concentrations and small  $T_c$  values.<sup>3</sup> A number of diverse models have been developed to account for the oxygen isotope effect in HTSC. However, there is no consensus as to which model is correct.

Unlike the oxygen isotope effect data, contradictory results exist in the case of the copper isotope effect. For example  $\alpha_{\text{Cu}}$  has been reported to be  $-0.17$  in  $\text{YBa}_2\text{Cu}_3\text{O}_{6.41}$  with  $T_c = 49.5$  K,<sup>4</sup>  $+0.38$  in  $\text{YBa}_2\text{Cu}_3\text{O}_{7-\delta}$  with  $T_c \approx 48$  K,<sup>5</sup> and  $+0.22$  in  $\text{Y}_{0.6}\text{Pr}_{0.4}\text{Ba}_2\text{Cu}_3\text{O}_7$  with  $T_c = 45$  K.<sup>6</sup> Negative Cu isotope effect exponents were found in  $\text{YBa}_2\text{Cu}_3\text{O}_{7-\delta}$  for all  $\delta$  values<sup>4</sup> while positive values were found in  $\text{YBa}_2\text{Cu}_3\text{O}_{7-\delta}$  for  $T_c < 90$  K and for various substituted forms of  $\text{YBa}_2\text{Cu}_4\text{O}_8$ .<sup>6</sup> Further experimental research is clearly required to resolve these inconsistencies.

Isotope effect measurements in the normal state are also of interest in relation to the normal-state pseudogap above  $T_c$  which has a profound effect on most physical properties and is also widely regarded as being linked to the pairing mechanism. In particular, the pseudogap causes the spin susceptibility to decrease rapidly with decreasing temperature as evidenced by a reduction in the Knight shift or the bulk susceptibility. There is considerable disagreement in the lit-

erature concerning the origin and nature of the normal-state pseudogap.<sup>7</sup> While many recent papers have pointed to the possible link between the pseudogap and incoherent pairing correlations existing well above  $T_c$ ,<sup>8</sup> we have argued strongly against this view.<sup>9</sup>

Our previous high-resolution  $^{89}\text{Y}$  nuclear-magnetic-resonance (NMR) measurements on  $^{16}\text{O}$  and  $^{18}\text{O}$  exchanged  $\text{YBa}_2\text{Cu}_4\text{O}_8$  found no isotope effect in the normal-state Knight shift data for temperatures above 150 K.<sup>9</sup> This would appear to be inconsistent with previous precursor pairing models in which the pairing and pseudogap correlations are essentially identical. However, a recent  $^{63}\text{Cu}$  nuclear quadrupole resonance (NQR) study on  $^{16}\text{O}$  and  $^{18}\text{O}$  exchanged  $\text{YBa}_2\text{Cu}_4\text{O}_8$  indicated an isotope effect in  $1/^{63}\text{T}_1 T$  for temperatures up to 350 K which is comparable to that observed in  $T_c$ .<sup>10</sup> This led the authors to conclude a common origin between the superconducting gap and the "spin gap." Noting our own null effect in the Knight shift the authors further concluded a distinction between the response at  $\mathbf{q} = \mathbf{Q}_{\text{AF}} \equiv (\pi, \pi)$  (from the spin-lattice relaxation rate,  $^{63}\text{T}_1$ ) and the  $\mathbf{q} = (0, 0)$  response (from the  $^{89}\text{Y}$  Knight shift). We conveniently restate their conclusion as a distinction between the spin gap and the pseudogap (a gap in the quasiparticle spectrum).

In this paper we question these conclusions. We report Raman, susceptibility, and  $^{89}\text{Y}$  NMR measurements of both the oxygen and copper isotope effects in  $\text{YBa}_2\text{Cu}_4\text{O}_8$ . This compound is ideal for such studies because it is underdoped and highly stoichiometric.

$\text{YBa}_2\text{Cu}_4\text{O}_8$  ceramic samples were prepared from isotopically pure  $^{65}\text{Cu}$  or  $^{63}\text{Cu}$  metal. CuO powder from each isotope was obtained by dissolving the Cu metal in nitric acid followed by decomposing the nitrate at 700 °C in air. Phase pure  $\text{YBa}_2\text{Cu}_4\text{O}_8$  polycrystalline samples were synthesized by standard solid-state reaction at 945 °C and 60 bars oxygen

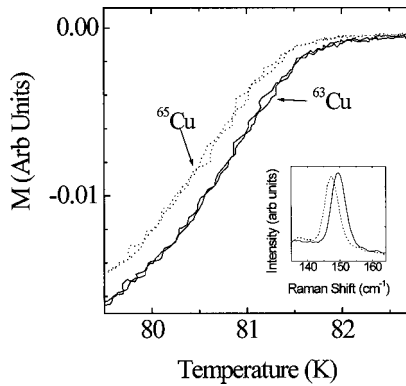


FIG. 1. Plot of the magnetization against temperature for  $\text{YBa}_2^{63}\text{Cu}_4\text{O}_8$  (solid curves) and for  $\text{YBa}_2^{65}\text{Cu}_4\text{O}_8$  (dashed curves). Inset: plot of the Cu2 mode in the Raman spectra for  $\text{YBa}_2^{63}\text{Cu}_4\text{O}_8$  (solid curve) and  $\text{YBa}_2^{65}\text{Cu}_4\text{O}_8$  (dashed curve) samples.

pressure. X-ray diffraction confirmed that the samples were single phase. The oxygen isotope exchange technique is described elsewhere.<sup>9</sup>

Zero-field-cooled temperature-dependent susceptibility data were obtained using a vibrating sample magnetometer with an applied field of  $5 \times 10^{-4} T$ . Raman measurements were made at room temperature using a backscattering geometry with the  $\lambda = 514.5$  nm of an argon ion laser.

The  $^{89}\text{Y}$  NMR data were obtained for temperatures ranging from 130 to 350 K using a Doty Super-VT Penguin probe in a Varian Unity 500 spectrometer with a 11.74 T superconducting magnet. Magic angle spinning (MAS) at frequencies greater than 2.5 kHz was used to remove dipole-dipole coupling and hence significantly reduce the width of the NMR resonance. The exceptionally narrow linewidth ( $\sim 100$  Hz) and accurate temperature control ( $< 0.2$  K) allows very precise determination of the shifts which were referenced to 1 molar aqueous solution of  $\text{YCl}_3$ . Moreover, both the selected temperature and the selected isotope for any one measurement were chosen more or less at random, thus eliminating any systematic effect due to possible heating from sample spinning. The data were obtained using the single  $90^\circ$  pulse technique.

We consider first the isotope effects in  $T_c$ . Figure 1 shows the susceptibility data from repeated measurements on  $\text{YBa}_2^{63}\text{Cu}_4\text{O}_8$  (solid lines) and  $\text{YBa}_2^{65}\text{Cu}_4\text{O}_8$  (dashed lines) samples where it can be seen that  $T_c$  is smaller by  $\Delta T_c = -(0.25 \pm 0.06)$  K in the sample with the larger Cu atomic weight. Taking  $T_c = 81.6$  K we find  $\alpha_{\text{Cu}} = 0.098 \pm 0.024$ , a value comparable to that observed by Morris *et al.*<sup>6</sup> in  $\text{Y}_{1-x}\text{Pr}_x\text{Ba}_2\text{Cu}_4\text{O}_8$  and  $\text{Y}_{1-x}\text{Pr}_x\text{Ba}_2\text{Cu}_3\text{O}_7$  with similar  $T_c$  values and approximately a factor of two less than that observed by Zhao *et al.*<sup>5</sup> in  $\text{YBa}_2\text{Cu}_3\text{O}_{7-\delta}$  with  $T_c \approx 72$  K. Both the magnitude and sign are different from those observed by Franck *et al.*<sup>4</sup> in  $\text{YBa}_2\text{Cu}_3\text{O}_{7-\delta}$  with similar  $T_c$  values. The origin of this difference is not clear but it could arise in the oxygenation processes for  $\text{YBa}_2\text{Cu}_3\text{O}_{7-\delta}$  from differences in the diffusion coefficient if the samples are not at equilibrium. Because of the rigid stoichiometry, we believe the measurements on the  $\text{YBa}_2\text{Cu}_4\text{O}_8$  system to be more reliable. Raman measurements, shown in the inset to Fig. 1, reveal that each of our samples contain either 100%  $^{63}\text{Cu}$  or 100%  $^{65}\text{Cu}$ . Here it can be seen that the Cu mode from Cu2 on the  $\text{CuO}_2$

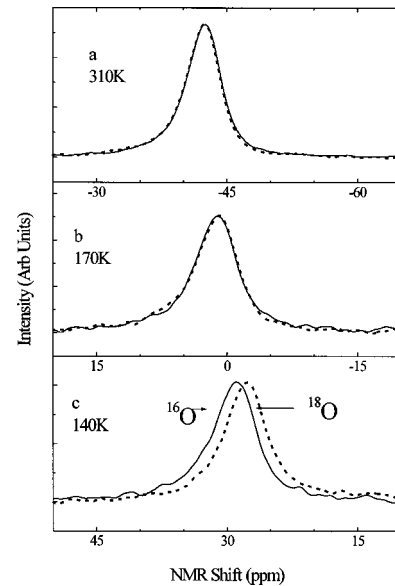


FIG. 2. Plot of the  $^{89}\text{Y}$  NMR spectra at the temperatures indicated for  $^{16}\text{O}$  exchanged  $\text{YBa}_2^{63}\text{Cu}_4\text{O}_8$  (solid curves) and  $^{18}\text{O}$  exchanged  $\text{YBa}_2^{65}\text{Cu}_4\text{O}_8$  (dashed curves).

planes at  $149.5$   $\text{cm}^{-1}$  in  $\text{YBa}_2^{63}\text{Cu}_4\text{O}_8$  shifts down to  $147.3$   $\text{cm}^{-1}$  in  $\text{YBa}_2^{65}\text{Cu}_4\text{O}_8$ . The fractional change in the mode position of 1.47% equals, within errors, the expected value from  $1 - \sqrt{63/65}$  of 1.55%. A similar shift is observed in the Cu1 mode from Cu in the  $\text{CuO}$  ribbons. We note that the assignment of this mode to a pure Cu mode is consistent with a (i) Raman study on  $\text{YBa}_2^{63}\text{Cu}_3\text{O}_{7-\delta}$  and  $\text{YBa}_2^{65}\text{Cu}_3\text{O}_{7-\delta}$  (Ref. 11) and (ii) the absence of an oxygen-isotope-induced shift in the frequency of this mode.<sup>11</sup> For the oxygen isotope effect in  $T_c$  for  $\text{YBa}_2\text{Cu}_4\text{O}_8$ , we have previously found  $\alpha_o = (0.076 \pm 0.010)$  K.<sup>9</sup> This is comparable to  $\alpha_o$  previously found by Zhao *et al.* in  $\text{YBa}_2\text{Cu}_3\text{O}_{7-\delta}$ ,<sup>5</sup> Morris *et al.* in  $\text{Y}_{0.8}\text{Pr}_{0.2}\text{Ba}_2\text{Cu}_3\text{O}_7$  (Ref. 5), and more recently Raffa *et al.* in  $\text{YBa}_2\text{Cu}_4\text{O}_8$ .<sup>10</sup> Thus both the copper and oxygen isotope effects are of similar magnitude and sign. This result is important because it shows that both the oxygen and copper vibrational modes contribute equally to  $T_c$  which is inconsistent with models based solely on one of the higher-frequency oxygen vibrational modes.

Turning now to the pseudogap, we show in Fig. 2 that an oxygen isotope effect in the normal-state  $^{89}\text{Y}$  NMR spectra is only observed at low temperatures. These results are similar to those observed in  $\text{YBa}_2\text{Cu}_4\text{O}_8$  with naturally occurring Cu (69.09%  $^{63}\text{Cu}$  and 30.91%  $^{65}\text{Cu}$ ).<sup>9</sup> On the other hand, we show in Fig. 3 that the copper isotope effect in the normal-state is different from the oxygen isotope effect. In contrast to the oxygen isotope spectra in Fig. 2, we find only a small shift at 140 K but it is in the *opposite* direction to the oxygen isotope effect. This is seen more clearly in Fig. 4(a) where we plot the change in the position of the  $^{89}\text{Y}$  NMR MAS peak,  $\Delta K_s$ , against temperature for all our isotope effect measurements. There is no oxygen or copper isotope effect for temperatures greater than 150 K. Below 150 K, our new data confirms that  $\Delta K_s$  is positive for the oxygen isotope effect, as previously observed,<sup>9</sup> while  $\Delta K_s$  is negative for the copper isotope effect.

To understand and model this data we must first consider

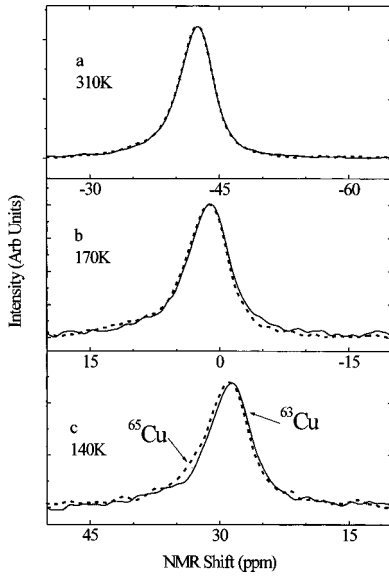


FIG. 3. Plot of the  $^{89}\text{Y}$  NMR spectra at the temperatures indicated for  $\text{YBa}_2^{63}\text{Cu}_4\text{O}_8$  (solid curves) and for  $\text{YBa}_2^{65}\text{Cu}_4\text{O}_8$  (dashed curves).

the origin of the  $^{89}\text{Y}$  NMR shift. Using the Mila-Rice Hamiltonian<sup>12</sup> it was possible to show that the NMR shift can be expressed as a linear function of the static spin susceptibility.<sup>13</sup> Within this model, there is hyperfine coupling from Cu spins on the eight nearest-neighbor Cu sites to the  $^{89}\text{Y}$  nucleus.

We show in Fig. 4(b) that  $-^{89}K$  (solid curve) decreases with decreasing temperature. This temperature dependence, in particular the suppression of  $\chi_s$  on cooling, has previously been attributed to the normal-state pseudogap.<sup>14</sup> Modeling of the normal-state pseudogap is complicated by recent observations of anisotropic filling in of the normal-state pseudogap with increasing temperature.<sup>15</sup> To be able to model the isotope effect in the normal state, we use a scaling

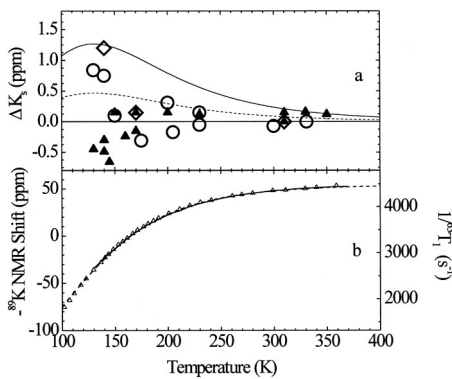


FIG. 4. (a)  $T$  dependence of the isotope-induced change in the Knight shift  $\Delta K_s$  obtained from  $^{89}\text{Y}$  NMR measurements for: oxygen isotope effect in  $\text{YBa}_2\text{Cu}_4\text{O}_8$  with natural copper [open circles (Ref. 9)], oxygen isotope effect in  $\text{YBa}_2^{65}\text{Cu}_4\text{O}_8$  (open diamonds) and the copper isotope (filled up triangles). The solid (dashed) curve is the shift expected if  $\alpha_E = \alpha_{T_c}$  for oxygen (for copper). (b) Plot of the  $T$  dependence on the  $^{89}\text{Y}$  NMR shift (left axis and solid curve) and the  $1/^{63}T_1$  data for Raffa *et al.* (Ref. 10) against temperature (right axis and open up triangles). The dashed curve is the scaling curve described in the text.

curve that fits the NMR data from a number of HTSC over a wide range of hole concentrations.<sup>14</sup> To justify a functional form for the scaling curve we start with the Pauli spin susceptibility,  $\chi_s = \mu_B^2 \int N(E) (-\partial f / \partial E) dE$ , where  $N(E)$  is the density of states (DOS) and  $f(E)$  is the Fermi function, and assume a triangular density of states that fills in with increasing temperature. This leads to

$$^{89}K = N(E_F) [1 - z \times \tanh^n(1/z) \ln(\cosh(1/z))] + ^{89}\sigma, \quad (1)$$

where  $N(E_F)$  is the DOS at the Fermi level in the absence of the pseudogap,  $z = 2k_B T / E_g$ ,  $^{89}\sigma$  is the temperature-independent  $^{89}\text{Y}$  chemical shift, and  $E_g$  is the pseudogap energy defined as the gap edge. This scaling curve and the associated density of states contain the essential experimental observations of a linear DOS, a linear-in-temperature NMR shift at low temperatures and a temperature-independent NMR shift and  $S/T$  at high temperatures,<sup>16</sup> where  $S$  is the electronic entropy. We show in Fig. 4(b) by the dashed curve that this scaling curve does indeed fit the data with  $E_g/k_B = 418$  K and  $n = 4.55$ . We emphasize that, without introducing a specific model, scaling of the  $^{89}\text{Y}$  NMR data above  $T_c$  shows that it is only the hole-concentration dependence of the pseudogap energy and not its absolute magnitude that can be determined. This is obvious because one curve must be chosen to scale the other curves against. Thus using a different form for the density of states will result in a different absolute magnitude. However, it is  $\Delta E_g / E_g$  that is important for studying the isotope effect in the normal-state pseudogap and not the absolute magnitude.

If an isotope effect existed in the normal-state pseudogap we could define a coefficient  $\alpha_{E_g} = -d \ln(E_g) / d \ln M$  and hence  $\Delta E_g / E_g = -\alpha_{E_g} \Delta M / M$ . Using the experimental observation that  $^{89}K_s = ^{89}K_s(z)$ , where  $z = 2k_B T / E_g$ , it can easily be shown that an isotope effect in  $E_g$  will lead to a change in the  $^{89}\text{Y}$  NMR Knight shift of  $\Delta ^{89}K_s = (-z \partial K_s / \partial z) \Delta E_g / E_g$  and hence  $\Delta ^{89}K_s = (-z \partial K_s / \partial z) \alpha_{E_g} \Delta M / M$  which removes the dependence on the absolute magnitude of the normal-state pseudogap. Using Eq. (1) for the scaling function and our experimental  $\alpha_o$  and  $\alpha_{\text{Cu}}$  values we show in Fig. 4(a) that the data cannot be accounted for by assuming an isotope effect in the normal-state pseudogap with the same value as that in  $T_c$ . Here the solid curve denotes the calculated oxygen isotope effect and the dashed curve is the calculated copper isotope effect.

Recent NQR oxygen isotope effect measurements on  $\text{YBa}_2\text{Cu}_4\text{O}_8$  showed values of  $1/^{63}T_1 T$  that were slightly larger for  $T < 350$  K in the  $^{18}\text{O}$  exchanged sample than for the  $^{16}\text{O}$  exchanged sample.<sup>10</sup> Moreover, NQR measurements of  $T_{2G}$ , where  $T_{2G}$  is the Gaussian component of the copper spin-spin-relaxation time, at 100 K showed no discernible oxygen isotope dependence. These results were analyzed in terms of an isotope effect in a spin gap with the same magnitude as the isotope effect in  $T_c$  where, in the authors' view, the spin gap could possibly be due to a charge-density-wave instability opening at 180 K.<sup>10</sup>

First, we wish to emphasize again the close relationship between  $^{89}K_s$  and  $1/^{63}T_1$ . We have previously shown that a good correlation exists between  $^{89}K_s$  and the  $1/^{63}T_1$  (Ref. 14) where we used our  $^{89}K_s$  data and the  $1/^{63}T_1$  of Curro

*et al.*<sup>17</sup> and Corey *et al.*<sup>18</sup> We now show in Fig. 4(b) that this correlation is even better when we plot the high-precision  $1/^{63}T_1$  data of Raffa *et al.*<sup>10</sup> and our high-precision  $^{89}\text{Y}$  NMR data.

We note that  $1/^{63}T_1$  probes the imaginary part of the dynamic spin susceptibility about  $\mathbf{q}=\mathbf{Q}_{\text{AF}}\equiv(\pi,\pi)$  while the NMR shift probes the real part of the dynamical spin susceptibility at  $\mathbf{q}=(0,0)$ . The almost exact correspondence between  $1/^{63}T_1$  and  $^{89}K_s$  again shows that the spin response is the same at  $\mathbf{q}=(0,0)$  and  $\mathbf{q}=(\pi,\pi)$  and there is no distinct lower crossover temperature at which a gap opens up at  $\mathbf{q}=(\pi,\pi)$  as is suggested by the peak in  $1/^{63}T_1T$ . We previously showed that using the Mila-Rice Hamiltonian and the phenomenological dynamical spin susceptibility of Millis, Monien, and Pines (MMP) can lead to a direct correspondence between  $1/^{63}T_1$  and  $K_s$  provided that the dynamical spin susceptibility,  $\chi_s(\mathbf{q},\omega)$ , is proportional to the static spin susceptibility,  $\chi_s(T)$ , as originally proposed by MMP.<sup>13</sup> Using the Mila Rice form factors in the limit of  $\xi^2\gg 1$  leads to  $1/^{63}T_1T=a_1\chi_s(T)/\omega_{sf}(T)$ , where  $a_1$  is a constant,  $\xi$  is the antiferromagnetic correlation length, and  $\omega_{sf}$  is the paramagnon frequency. Taking  $\omega_{sf}$  as being proportional to temperature results in a  $1/^{63}T_1$  being directly proportional to  $\chi_s$  as is observed. The precise correspondence between  $1/^{63}T_1$  and  $^{89}K_s$  shown in Fig. 4(b) would lead one to expect the same isotope effect in each of these parameters.

Secondly, Ohno and Asayama<sup>19</sup> have recently analyzed the data of Raffa *et al.* and shown that  $1/^{63}T_1$  plotted against  $T/T_c$  for the  $^{18}\text{O}$  and  $^{16}\text{O}$  samples falls on the same curve

over the entire temperature range. This has been interpreted in terms of an isotope effect in the characteristic energy of the antiferromagnetic spin fluctuations without any isotope effect in a ‘‘spin gap.’’ This interpretation follows from the expansion of  $1/^{63}T_1T$ , leading to  $1/^{63}T_1T=a_1\chi_s(T)/\omega_{sf}(T/T_c)$ , where the isotope effect is in  $\omega_{sf}$  rather than  $\chi_s(T)$ . We may similarly understand why the copper  $T_{2G}$  at 100 K does not show an oxygen isotope effect.<sup>10</sup> Using the Mila-Rice Hamiltonian and  $\chi_s(\mathbf{q},\omega)$ , where the copper  $T_{2G}$  predominantly samples the real part of the dynamic spin susceptibility about  $\mathbf{q}=(\pi,\pi)$ , we find in the limit of  $\xi^2\gg 1, 1/T_{2G}=a_2\xi(T)\chi_s(T)$ , where  $a_2$  is a constant. Therefore, the absence of an isotope effect in  $\chi_s(T)$  automatically leads to the absence of an isotope effect in  $T_{2G}$ .

In conclusion, we have shown that there is no oxygen or copper isotope effect in the normal state of the underdoped  $\text{YBa}_2\text{Cu}_4\text{O}_8$  superconductor for temperatures above 150 K. Below 150 K small oxygen and copper isotope effects appear but they are of opposite sign while the oxygen and copper isotope effects in  $T_c$  are both positive. This further emphasizes that the pseudogap is unlikely to be related to superconducting pairing correlations.

We gratefully acknowledge C. Bernhard and M. Cardona for supplying the copper isotopes and for helpful discussions. We acknowledge funding from the New Zealand FRST, The Royal Society of New Zealand, and the Alexander von Humboldt Foundation.

- 
- <sup>1</sup>J. Bardeen, Phys. Rev. **79**, 167 (1950).  
<sup>2</sup>G. Gladstone, M. A. Jensen, and J. R. Schrieffer, in *Superconductivity*, edited by R. D. Parks (Marcel Dekker Inc., New York, 1969), p. 767.  
<sup>3</sup>J. R. Franck, in *Physical Properties of High Temperature Superconductors IV*, edited by D. M. Ginsberg (World Scientific, Singapore, 1994), p. 189.  
<sup>4</sup>J. P. Franck and D. D. Lawie, J. Supercond. **8**, 591 (1995).  
<sup>5</sup>G. Zhao, V. Kirtikar, K. K. Singh, A. P. B. Sinha, D. E. Morris, and A. V. Inyushkin, Phys. Rev. B **54**, 14 956 (1996).  
<sup>6</sup>D. E. Morris, A. P. B. Sinha, V. Kirtikar, and A. V. Inyushkin, Physica C **298**, 203 (1998).  
<sup>7</sup>T. Timusk and B. Statt, Rep. Prog. Phys. **62**, 61 (1999).  
<sup>8</sup>V. J. Emery and S. A. Kivelson, Nature (London) **374**, 434 (1993).  
<sup>9</sup>G. V. M. Williams, J. L. Tallon, J. W. Quilty, H. J. Trodahl, and N. E. Flower, Phys. Rev. Lett. **80**, 377 (1998).  
<sup>10</sup>F. Raffa, T. Ohno, M. Mali, D. Brinkmann, K. Conder, and M. Eremin, Phys. Rev. Lett. **81**, 5912 (1998).  
<sup>11</sup>R. Henn, T. Strach, E. Schönherr, and M. Cardona, Phys. Rev. B **55**, 3285 (1997).  
<sup>12</sup>F. Mila and T. M. Rice, Physica C **157**, 561 (1989).  
<sup>13</sup>A. J. Millis, H. Monien, and D. Pines, Phys. Rev. B **42**, 167 (1990).  
<sup>14</sup>G. V. M. Williams, J. L. Tallon, and J. W. Loram, Phys. Rev. B **58**, 15 053 (1998).  
<sup>15</sup>M. R. Norman, H. Ding, M. Randeria, J. C. Campuzano, T. Yokoya, T. Takeuchi, T. Takahashi, T. Mochiku, K. Kadowaki, P. Guptasarma, and D. G. Hinks, Nature (London) **392**, 157 (1998).  
<sup>16</sup>J. L. Tallon, J. W. Loram, and G. V. M. Williams, J. Phys. Chem. Solids **59**, 2091 (1998).  
<sup>17</sup>N. J. Curro, T. Imai, C. P. Slichter, and B. Dabrowski, Phys. Rev. B **56**, 877 (1997).  
<sup>18</sup>R. L. Corey *et al.*, Phys. Rev. B **53**, 5907 (1996).  
<sup>19</sup>T. Ohno and K. Asayama, Phys. Lett. A **258**, 367 (1999).